Inhibition of KIF20A by Transcription Factor IRF6 Affects the Progression of Renal Clear Cell Carcinoma

Xinwei Ma
the second affiliated hospital of soochow university
Xiaoqi Wang
the first affiliated hospital of Anhui University of science and technology
Qian Dong
suzhou science and technology town hospital
Hongquan Pang
Suzhou Science and Technonlgy Town Hospital
Jianming Xu
Suzhou Science and Technology Town Hospital
Junkang Shen (shengjunk@126.com)
The second affiliated hospital of soochow university https://orcid.org/0000-0002-1757-0056
Jianbing Zhu
Suzhou Science and Technology Town Hospital

Primary research

Keywords: renal clear cell carcinoma, IRF6, KIF20A, prognosis, early diagnostic target

Posted Date: December 31st, 2020

DOI: https://doi.org/10.21203/rs.3.rs-136418/v1

Abstract

Background: Renal clear cell carcinoma (ccRCC) is one of the most common malignant tumors, and its incidence is increasing year by year. IRF6 plays an important role in the occurrence of tumors, but the expression of IRF6 in ccRCC has not been reported so far.

Methods: The expression of IRF6 and KIF20A in ccRCC was predicted by GEPIA and HAP database. In addition, the GEPIA database predicted the relationship between the expression of IRF6 and KIF20A and the pathological staging, overall survival, and disease-free survival of ccRCC. The possible binding sites of IRF6 and KIF20A promoters were predicted by JASPAR database and verified by luciferase and ChIP experiments. The specific effects of IRF6 on proliferation invasion and apoptosis of ccRCC were subsequently examined at the cellular level. The expression of IRF6 and KIF20A in ccRCC cell lines was detected by RT-qPCR and western blot. Cell transfection techniques were used to construct IRF6 and KIF20A overexpressed or interfering plasmids. CCK-8 and clone formation assays were used to detect cell activity. Apoptosis was detected by TUNEL assay. Wound healing and Transwell assays detected the ability of cell migration and invasion, respectively.

Results: The database predicted that IRF6 expression was down-regulated in renal carcinoma tissues and correlated with poor prognosis. Cell experiments showed that overexpression of IRF6 inhibited proliferation, invasion and migration of ccRCC. In addition, the database predicted that KIF20A was up-regulated in renal carcinoma tissues and associated with prognosis, and cell experiments demonstrated that interference with KIF20A inhibited proliferation, invasion, and migration of ccRCC. Finally, we confirmed that KIF20A is a functional target of IRF6, and KIF20A partially reverses the effects of IRF6 on the proliferation, invasion and migration of ccRCC.

Conclusion: Inhibition of KIF20A by transcription factor IRF6 affects the cell proliferation, invasion, migration of renal clear cell carcinoma.

Introduction

Renal cell carcinoma, also known as kidney cancer, is one of the top ten cancers in the world, with its incidence accounting for 2% of the total number of cancers worldwide and showing an increasing trend year by year (1). Clear cell carcinoma of kidney (ccRCC) originated from proximal renal tubular cells is the most common renal carcinoma, accounting for 70%~80% of renal carcinoma (2). In the early stage of ccRCC, there are basically no symptoms (3). Therefore, more and more researches focus on exploring the key molecules for the diagnosis and treatment of clear cell carcinoma of the kidney.

Interferon Regulatory Factor 6 (IRF6) is an important member of the interferon regulatory factor family. The expression product of IRF6 is transcription factor, which can regulate cell proliferation, cycle and differentiation (4–6). IRF6 plays an important role in tumor genesis and inhibition. Study has shown that IRF6 expression is down-regulated in gastric cancer and is associated with poor prognosis, which may be caused by overexpression of ZEB1 and DNA methylation of IRF6 promoter (7). IRF6 is down-regulated in

highly metastatic nasopharyngeal carcinoma cells, and the increased expression of IRF6 inhibits cell proliferation, growth, and tumor stem cell dryness, and enhances the chemotherapeutic sensitivity of the cells (8). The expression of IRF6 in ccRCC has not been reported.

The binding sites of IRF6 and KIF20A were predicted by JASPAR2020 database. Through TCGA database mining, Wei et al. found that KIF20A was up-regulated in ccRCC tissues, and its expression was significantly correlated with overall survival rate and relapse-free survival rate, and it was the hub gene associated with metastasis (9). Six hub genes (CCNB2, CDC20, CEP55, KIF20A, TOP2A and UBE2C) of ccRCC were identified through the co-expression network of GSE40435 and GSE53757 database and PPI, which were highly correlated with pathological stage and poor prognosis (10). GSE53757 database showed that KIF20A was highly expressed in ccRCC and significantly correlated with prognosis. PCR assay was used to detect the expression profile of 44 patients with ccRCC and the significant upregulation of KIF20A was verified (11). However, none of these studies functionally verified the role of KIF20A overexpression and knockout in ccRCC.

So in our article, we investigated the role and mechanism of IRF6 in the malignant progression of ccRCC through database analysis and in vitro and in vivo experimental verification.

Materials And Methods

Database selection and analysis

We used the databases: Gene Expression Profiling Interactive Analysis (GEPIA: http://gepia.cancer-pku.cn) to perform validation of cancer specific expression and prognosis of the IRF6 genes and KIF20A genes (28407145) .

In addition, in the light of the expression of Hub genes and its relationship with pathological stage of tumor in GEPIA, one-way ANOVA statistical analysis was used. The overall survival (OS) and disease free survival analyses of the hub genes were performed using the Mantel-Cox test survival method in GEPIA.

We used the databases: The Human Protein Atlas (HPA: http://www.proteinatlas.org/) to perform the expression of IRF6 and KIF20A in renal carcinoma tissues.

We used the JASPAR database (http://www.jaspar.genereg.net)) to predict the possible binding sites of the IRF6 and KIF20A promoters.

Animals

6 healthy female BALB/C nude mice aged 6-8 weeks were selected from Animal Experimental Center. All animal experiments in the present study were approved by the Ethics Committee of The second affiliated hospital of soochow university. All methods were performed in accordance with the United States Public Health Services Guide for the Care and Use of Laboratory Animals, and all efforts were made to minimize the suffering and number of animals used in the present study. The nude mice were raised in SPF

conditions. 786-O cells at logarithmic growth stage were inoculated subcutaneously at the right back near the upper limb of nude mice by 6×10^7 unit/ml. Mice were treated for 4 weeks for modeling.

Cell culture

Renal tubular epithelial cell HK2 cell and renal clear cell carcinoma cell line OS-RC-2, 769-P, CaKi-1, UM-RC-2 and 786-O were purchased from the Cell Resource Center of Shanghai Institutes for Biological Sciences (Chinese Academy of Sciences, Shanghai, China). Cells were cultured in RPMI1640 medium containing 10% fetal bovine serum (FBS), and 100μg/ml streptomycin at 37°C with 5% CO_2 in a humid incubator.

RT-qPCR

Total RNA was extracted from the cells using TRIzol reagent (Invitrogen, Waltham, Massachusetts). The PrimerScript Real-time reagent kit (TaKaRa, Kusatsu, Shiga, Japan) was performed for total RNA reverse transcription, and then SYBR Premix Ex TaqTM II (TaKaRa, Japan) was used for the quantitation analysis of the expression of IRF6 and KIF20A. We designed the stem-loop with IRF6 and KIF20A sequence (which was used to the primer of reverse transcription) and used stem-loop to complete reverse transcription. The primer sequences for primer source were performed as follows: IRF6: Forward: 5’ CAAAACTGAACCCCTGGAGATGGA 3’ Reverse: 5’- CCACGGTACTGAAAC TTGATGTCC-3’; KIF20A: Forward: 5'-TGCTGTCCGATGACGATGTC-3' Reverse: 5'-AGGTTCTTGCGTACCACAGAC-3'; GAPDH: Forward: 5'-AGGTTCTTGCGTACCACAGAC-3' Reverse: 5'-GCCATCACGCCACAGTTTC-3'.

Western blot

Lysis buffer (Sigma, USA) was added to the cells to isolate total protein. The concentration of protein was determined using a bicinchoninic acid assay protein assay kit. Proteins (25 μg/lane) were separated by SDS-10% polyacrylamide gel (Bio-Rad, Hercules, CA) and transferred to membrane of polyvinylidene fluoride (Thermo Fisher Scientific, Waltham, MA). Membranes were then blocked with 5% milk in Tris-buffered saline/Tween-20 for 1 h at room temperature, and then probed overnight at 4°C with the following primary antibodies: anti-IRF6 (1:1000; ab123880; Abcam, Cambridge, MA), anti- KIF20A (1:1000; ab7091; Abcam, Cambridge, MA) (Santa Cruz Biotechnology, Santa Cruz, CA), and anti-GAPDH (ab75478; Abcam, Cambridge, MA). After washing, blots were incubated with the appropriate HRP-conjugated secondary antibody for 2 h at room temperature. Proteins were detected with the enhanced chemiluminescence detection system (Thermo Fisher Scientific, Waltham, MA). The protein bands were visualized using the ChemiDoc XRS System (Bio-Rad), and Image J software were used to detect the blots.

Cell transfection

Overexpression (Oe)-IRF6, Oe-KIF20A, shRNA-IRF6, shRNA-KIF20A and the negative control (NC) were synthesized by GenePharma Co. (Shanghai, China). . All cell transfections were conducted by

using Lipofectamine 3000 reagent (Invitrogen, Carlsbad, CA, USA) following the manufacturer's protocol.

CCK-8

786-O cells (1×10^5) were inoculated into 96-well plates. The cells were treated accordingly and at 24, 48 and 72 h time intervals post-transfection, 10 μl CCK-8 solution (Beyotime Institute of Biotechnology) was added to each well, and the plates were then incubated for 48 h at 37°C. Optical density (OD) values at 450 nm were determined using an ELx808 absorbance microplate reader (BioTek Instruments, Inc., Winooski, VT, USA).

Colony formation assays

786-O cells (1×10^6) were inoculated into 6-well plates and transfected for 48 h. Then, the cells were cultured for 14 d at 37°C. After this, cells were stained with 10% Giemsa (Merck, Germany) for 30 min. Colonies containing ≥50 cells were counted under a microscope (Olympus, Japan). Each experiment was repeated three times.

TUNEL Staining

For TUNEL staining, 786-O cells (1×10^6) were inoculated into 6-well plates and transfected for 48 h. Cells were fixed in freshly prepared 4 % methanol-free formaldehyde solution in PBS for 20 min at room temperature and permeabilized with 0.2 % Triton X-100 for 5 min. 786-O cells were labeled with fluorescein TUNEL reagent mixture for 60 min at 37 °C according to the manufacturer's suggested protocol. After that, slides were examined by fluorescence microscopy and the number of TUNEL-positive (apoptotic) cells was counted. DAPI was used to stain nucleus.

Wound healing

786-O cells (1×10^6) were inoculated into 6-well plates and transfected for 48 h. A wound was created by using a 100 μL pipette tip on the cell monolayer and images were taken at 0 h and 24 h to calculate the % of wound healing.

Transwell

The treated cells were inoculated into the upper chamber of 24-well Transwell chamber at the density of 2*105 cell/well. Matrigel glue was laid on the upper chamber and the culture medium with a volume of 600μL containing 10% FBS was added to the lower chamber. After 24 hours of incubation, carefully remove the Transwell chamber and fix it for 20 minutes with 4% polyformaldehyde solution. Then wash it with PBS solution, and wipe out the cells on the surface of the chamber with cotton swabs to crystallize. After purple staining, microscopic observation was carried out. Select six visual fields of each group to photograph and count, and calculate an average. The experiment was repeated independently for three times.

Luciferase assay

The luciferase activity was measured using a plate reader (BD bioscience), and normalized to the transfection efficiency by using a Renilla luciferase activity kit (pRL-TK). All procedures followed the manufacturers' instructions. All plasmids were constructed by Life Technologies Corporation (Carlsbad, CA).

Chromatin immunoprecipitation assay (ChIP)

Chromatin immunoprecipitation (ChIP) was carried out with a Magna Chromatin Immunoprecipitation kit (Millipore, Darmstadt, Germany). Immunoprecipitation was performed with anti-IRF6 antibody. The final purified DNA fragment was subjected to PCR analysis using Hot-Start Taq DNA polymerase (TaKaRa, Dalian, China; 32 cycles). PCR products were analyzed using gel electrophoresis. ChIP data were shown as the percentage of the input normalized to control purifications.

Immunohistochemical (IHC)

Xenograft tumors were collected and performed on paraffin-embedded sections. 4 μm-thick sections were deparaffinized, rehydrated and then immersed with 3% hydrogen peroxide for 10 min to quench endogenous peroxidase and labeled with antibodies at 4 °C overnight. The slides were stained with the secondary streptavidin-horseradish peroxidase-conjugated antibody (Santa Cruz Biotech, Santa Cruz, CA) for 1 h. The slides were then counterstained with hematoxylin for 30s and cover slipped.

Statistical analysis

Statistical calculations were performed using SPSS 13.0 software (SPSS, Inc., Chicago, IL, USA). The data are presented as the mean ± standard deviation from at least three independent experiments. Statistical analysis was performed by one-way ANOVA. $P<0.05$ was considered to indicate a statistically significant difference.

Results

Expression of IRF6 in renal carcinoma tissues and its relationship with prognosis

Through GEPIA database, we predict the expression of IRF6 in the tissues of patients with Kidney Chromophobe (KICH), Kidney renal clear cell carcinoma (KIRC), and Kidney renal papillatory cell carcinoma (KIRP).The expression of IRF6 was significantly decreased in KIRC patients (Fig. 1A). The HPA database results showed that the IHC results of IRF6 in renal carcinoma were negative (Fig. 1B). In addition, based on GEPIA data, we investigated that IRF6 expression was highly correlated with the pathological stage of renal clear cell carcinoma (Fig. 1C). As the tumor progression always affected the tumor prognosis, we also investigated the roles of IRF6 in ccRCC prognosis including overall survival time and disease free survival time. We found a shorter overall survival time (Fig. 1D) and disease-free survival time in patients with lower expression levels of IRF6 (Fig. 1E).

Overexpression of IRF6 inhibits proliferation, invasion and migration of ccRCC cells

We then validated our prediction at the cellular level. The results showed that the expression of IRF6 was significantly decreased in ccRCC cell lines (Fig. 2A and B). We selected 786-O cells for subsequent experiments. Cell transfection assay were used to interfere with IRF6 expression and overexpress IRF6. As shown in Fig. 2C and D, shRNA-IRF6 #2 had a better interference effect, so shRNA-IRF6 #2 was selected for subsequent experiments. The expression of IRF6 in cells increased significantly after overexpression of IRF6, indicating successful construction of overexpressed plasmid. We divided the cells into control, shRNA-NC, shRNA-IRF6, Oe-NC and Oe-IRF6. Cell proliferation was detected, and we found that the cell proliferation ability was significantly increased after the interference of IRF6 expression, while decreased after the overexpression of IRF6 (Fig. 3A and B). Apoptosis was detected by TUNEL assay, and the results showed that apoptosis was decreased in the shRNA-IRF6 group compared with the shRNA-NC group. Compared with the Oe-NC group, the apoptosis rate of the Oe-IRF6 group was increased (Fig. 3C). The results of wound healing experiment showed that after the interference of IRF6 expression, the cell migration ability was significantly increased. After the overexpression of IRF6, the cell migration ability was decreased (Fig. 4A and C). Transwell results showed the same trend with the result of wound healing experiment (Fig. 4B and D).

Expression of KIF20A in renal carcinoma tissues and its relationship with prognosis

Through the GEPIA database, we predicted the expression of KIF20A in the tissues of KICH, KIRC and KIRP patients, and the results were shown in Fig. 5A. The expression of KIF20A was significantly increased in KIRC patient tissues. HPA database results showed that KIF20A was highly expressed in renal cancer tissues (Fig. 5B). In addition, based on GEPIA data, we investigated that KIF20A expression was highly correlated with the pathological stage of renal clear cell carcinoma (Fig. 5C). We also investigated the roles of KIF20A in ccRCC prognosis including overall survival time and disease free survival time. We found a shorter overall survival time (Fig. 5D) and disease-free survival time in patients with higher expression levels of KIF20A (Fig. 5E).

Interference with KIF20A inhibits proliferation, invasion and migration of ccRCC cells

Our results showed that KIF20A was significantly increased in ccRCC cell lines (Fig. 6A and B). Cell transfection was used to disrupt KIF20A expression and construct KIF20A overexpressed plasmid. The transfection efficiency was detected by RT-qPCR and western blot. The interference effect of shRNA-KIF20A #2 was better, so shRNA-KIF20A #2 was selected for subsequent experiments. In addition, the expression of KIF20A in cells increased significantly after overexpression of KIF20A, indicating successful construction of the overexpressed plasmid (Fig. 6C and D). We divided the cells into control, shRNA-NC, shRNA-KIF20A, Oe-NC and Oe-KIF20A. Cell proliferation was detected, and we found that the cell proliferation ability decreased significantly after interfering of KIF20A expression, while the cell proliferation ability increased after the over-expression of KIF20A (Fig. 7A and B). Apoptosis was detected by TUNEL assay. Compared with the shRNA-NC, apoptosis was increased in the shRNA-KIf20A group. Compared with the Oe-NC, the apoptosis rate of the Oe-IRF6 group was decreased (Fig. 7C). The results of

wound healing (Fig. 8A and C) and transwell (Fig. 8B and D) showed that the cell migration and invasion decreased significantly after interfering of KIF20A, while increased after the over-expression of KIF20A.

KIF20A partially reverses the effects of IRF6 on the proliferation, invasion and migration of ccRCC cells

We used JASPAR database to predict that IRF6 and KIF20A promoters had binding sites (S1 and S2) (Fig. 9A). In addition, the GEPIA database showed that the expression level of IRF6 and KIF20A was highly correlated in KIRC (Fig. 9B). The expression of KIF20A in cells was significantly increased after interference with IRF6, while the expression of KIF20A was reversed after overexpression of IRF6 (FigC and D). Luciferase was used to detect the transcriptional activity of KIF20A promoter mutant in ccRCC cells (Fig. 9E). Finally, ChIP experiment verified the combination of IRF6 and KIF20A promoter (Fig. 9F). The above experimental results indicate that KIF20A is a functional target of IRF6.

We divided the cells into groups of shRNA-NC, shRNA-IRF6, shRNA-IRF6 + shRNA-NC and shRNA-IRF6 + shRNA-KIF20A and Oe-NC, Oe-IRF6, Oe-IRF6 + Oe-NC and Oe-IRF6 + Oe-KIF20A. We found that the expression of KIF20A increased after IRF6 interference, and the expression of KIF20A was reversed after further inhibition (Fig. 10A and B). After the overexpression of IRF6, the expression of KIF20A decreased, and after the further overexpression of KIF20A, the expression of KIF20A in the cells was reversed (Fig. 10C and D). We found that after IRF6 expression was interfered, the expression of KIF20A in cells was increased, cell viability was increased (Fig. 11A), cell proliferation ability was increased (Fig. 11B), apoptosis rate was decreased (Fig. 11C), cell migration ability and invasion ability (Fig. 12A) were increased. Further down-regulation of KIF20A expression in cells can inhibit cell proliferation, invasion and migration (Fig. 12B), and promote cell apoptosis. After the overexpression of IRF6, the expression of KIF20A in the cells decreased, and the cell viability decreased, cell proliferation ability decreased, migration and invasion ability decreased (Fig. 12B), and apoptosis rate increased. Further upregulation of KIF20A expression in cells can reverse these phenomena.

Overexpression of IRF6 inhibits the growth and metastasis of ccRCC in vivo

Mice were weighed and photographed before treatment (Fig. 13A). Then we stripped the tumor of the mice and weighed it, took pictures, and measured the tumor volume, as shown in Fig. 13B. we found that the tumor weight and volume decreased after the overexpression of IRF6. The expression of IRF6 and KIF20A in tumor tissues was detected by RT-QPCR (Fig. 13C) and western blot (Fig. 13D). After the overexpression of IRF6, the expression of IRF6 in tumor tissues increased, while the expression of KIF20A decreased. In addition, the expression of Ki67 was detected by IHC, and compared with Oe-NC, the expression of Ki67 in the Oe-IRF6 group was significantly decreased (Fig. 13E), indicating that the overexpression of IRF6 inhibited the proliferation of tumor cells in tumor-bearing mice.

Discussion

At present, molecular markers of renal clear cell carcinoma mainly include hypoxia-inducing factors HIF (12) and P53 (13), etc., but these molecular markers have certain limitations and cannot be widely used in

clinical practice. Therefore, finding new molecular markers can contribute to the early diagnosis and treatment of ccRCC.

IRF6 regulates craniofacial development and epidermal hyperplasia (5). In recent years, abnormal expression of IRF6 has been proved to cause a variety of diseases and regulate various physiological and biochemical processes (14). IRF6 plays an important role in the development of tumors. Down-regulation of IRF6 expression can inhibit the differentiation of primary human keratinocytes in vivo and in vitro, and promote the formation of RAS induced tumor (15). Martha L et al. showed that IRF6 was negatively associated with colorectal cancer risk and survival (16). However, the expression of IRF6 in ccRCC and its relationship with cancer prognosis have not been reported. In our paper, we found that IRF6 was significantly down-regulated in ccRCC tissues through GEPIA and HAP database. In addition, our basic experiments verified that IRF6 was down-regulated in ccRCC mice, and its expression was also significantly down-regulated in ccRCC cell lines.

Study has shown that IRF6 can be used as the downstream of Notch signaling pathway to regulate the proliferation and transformation of breast cancer cells, and can be used as a potential susceptibility marker of breast cancer (17, 18). In cutaneous squamous cell carcinoma, the expression of IRF6 is significantly decreased, and down-regulation of IRF6 can promote the invasion and growth of cancer cells (19). These results indicate that IRF6 can inhibit the proliferation, invasion and migration of tumor cells in a variety of tumors. In our paper, we also demonstrated that overexpression of IRF6 can significantly inhibit cell proliferation, invasion and migration, and promote apoptosis in ccRCC.

JASPAR predicts that IRF6 can target KIF20A. We also verified through relevant experiments that IRF6 can directly bind to the KIF20A promoter to regulate KIF20A expression. KIF20A is a member of Kinesin6 family, involved in key cell functions including intracellular activity of organelles and vesicles, spindle formation and cytokinesis (20). The expression and activity participate of KIF20A in the regulation of intracellular transport and cell division, and it plays an important role in the occurrence and development of cancer (21). In our study, we found that the expression of KIF20A was significantly increased in ccRCC, and interfering KIF20A can inhibit the proliferation, invasion and migration of cells. In addition, KIF20A can partially reverse the effects of IRF6 on the proliferation, invasion and migration of ccRCC cells.

Through the GEPIA, HAP and other databases, we found that the expression of IRF6 and KIF20A in ccRCC was significantly correlated with the pathological stage and overall survival rate of renal carcinoma patients. These results suggest that IRF6 and KIF20A are prognostic markers for poor survival in ccRCC patients.

Conclusion

In this paper, we demonstrate that the transcription factor IRF6 inhibits the expression of KIF20A and thus affects the proliferation, invasion, and apoptosis of ccRCC.

Declarations

Ethics approval and consent to participate

All animal procedures and experimental methods were approved by the Ethics Committee of The second affiliated hospital of soochow university, and were conducted in accordance with the ARRIVE guidelines.

Consent for publication

All the authors agreed to be published

Availability of data and material

We hereby undertake that all data and materials are available

Competing interests

There is no conflict of interest.

Funding

Suzhou key clinical diseases diagnosis and treatment technology special project (LCZX201930)

Suzhou Science and Technology Planed Projects (SYS2018010)

Suzhou High-tech Zone Medical and Health Technology Plan Project (2017Z005)

Authors' contributions

Junkang Shen and Jianbing Zhu contributed to conception and design, analysis and interpretation of the data, critically revised the article for important intellectual content. Xinwei Ma and Xiaoqi Wang contributed to design and analysis of the data, drafted and revised the manuscript. Qian Dong, Hongquan Pang and Jianming Xu substantially contributed to conception and design, acquisition, analysis, and interpretation of data; drafted and critically revised the article for important intellectual content. All authors approved the final version of the article and agreed to be accountable for all aspects of the work in ensuring that questions related to the accuracy or integrity of any part of the work are appropriately investigated and resolved.

Acknowledgement

No

References

1. Cheng SK, Chuah KL. Metastatic Renal Cell Carcinoma to the Pancreas: A Review. Arch Pathol Lab Med. 2016;140(6):598-602. doi: 10.5858/arpa.2015-0135-RS. PubMed PMID: 27232353.
2. Turajlic S, Swanton C, Boshoff C. Kidney cancer: The next decade. J Exp Med. 2018;215(10):2477-9. doi: 10.1084/jem.20181617. PubMed PMID: 30217855; PubMed Central PMCID: PMCPMC6170181.
3. Akhtar M, Al-Bozom IA, Al Hussain T. Molecular and Metabolic Basis of Clear Cell Carcinoma of the Kidney. Adv Anat Pathol. 2018;25(3):189-96. doi: 10.1097/PAP.0000000000000185. PubMed PMID: 29465421.
4. Taniguchi T, Ogasawara K, Takaoka A, Tanaka N. IRF family of transcription factors as regulators of host defense. Annu Rev Immunol. 2001;19:623-55. doi: 10.1146/annurev.immunol.19.1.623. PubMed PMID: 11244049.
5. Oberbeck N, Pham VC, Webster JD, Reja R, Huang CS, Zhang Y, et al. The RIPK4-IRF6 signalling axis safeguards epidermal differentiation and barrier function. Nature. 2019;574(7777):249-53. doi: 10.1038/s41586-019-1615-3. PubMed PMID: 31578523.
6. Degen M, Wiederkehr A, La Scala GC, Carmann C, Schnyder I, Katsaros C. Keratinocytes Isolated From Individual Cleft Lip/Palate Patients Display Variations in Their Differentiation Potential in vitro. Front Physiol. 2018;9:1703. doi: 10.3389/fphys.2018.01703. PubMed PMID: 30555344; PubMed Central PMCID: PMCPMC6281767.
7. Li D, Cheng P, Wang J, Qiu X, Zhang X, Xu L, et al. IRF6 Is Directly Regulated by ZEB1 and ELF3, and Predicts a Favorable Prognosis in Gastric Cancer. Front Oncol. 2019;9:220. doi: 10.3389/fonc.2019.00220. PubMed PMID: 31019894; PubMed Central PMCID: PMCPMC6458252.
8. Xu L, Huang TJ, Hu H, Wang MY, Shi SM, Yang Q, et al. The developmental transcription factor IRF6 attenuates ABCG2 gene expression and distinctively reverses stemness phenotype in nasopharyngeal carcinoma. Cancer Lett. 2018;431:230-43. doi: 10.1016/j.canlet.2017.10.016. PubMed PMID: 29111349.
9. Wei W, Lv Y, Gan Z, Zhang Y, Han X, Xu Z. Identification of key genes involved in the metastasis of clear cell renal cell carcinoma. Oncol Lett. 2019;17(5):4321-8. doi: 10.3892/ol.2019.10130. PubMed PMID: 30988807; PubMed Central PMCID: PMCPMC6447949.
10. Yuan L, Chen L, Qian K, Qian G, Wu CL, Wang X, et al. Co-expression network analysis identified six hub genes in association with progression and prognosis in human clear cell renal cell carcinoma (ccRCC). Genom Data. 2017;14:132-40. doi: 10.1016/j.gdata.2017.10.006. PubMed PMID: 29159069; PubMed Central PMCID: PMCPMC5683669.
11. Zhang H, Zou J, Yin Y, Zhang B, Hu Y, Wang J, et al. Bioinformatic analysis identifies potentially key differentially expressed genes in oncogenesis and progression of clear cell renal cell carcinoma. PeerJ. 2019;7:e8096. doi: 10.7717/peerj.8096. PubMed PMID: 31788359; PubMed Central PMCID: PMCPMC6883955.
12. Chen W, Hill H, Christie A, Kim MS, Holloman E, Pavia-Jimenez A, et al. Targeting renal cell carcinoma with a HIF-2 antagonist. Nature. 2016;539(7627):112-7. doi: 10.1038/nature19796. PubMed PMID: 27595394; PubMed Central PMCID: PMCPMC5340502.

13. Jing ZF, Bi JB, Li Z, Liu X, Li J, Zhu Y, et al. Inhibition of miR-34a-5p can rescue disruption of the p53-DAPK axis to suppress progression of clear cell renal cell carcinoma. Mol Oncol. 2019;13(10):2079-97. doi: 10.1002/1878-0261.12545. PubMed PMID: 31294899; PubMed Central PMCID: PMCPMC6763763.
14. Schutte BC, Saal HM, Goudy S, Leslie E. IRF6-Related Disorders. In: Adam MP, Ardinger HH, Pagon RA, Wallace SE, Bean LJH, Stephens K, et al., editors. GeneReviews((R)). Seattle (WA)1993.
15. Restivo G, Nguyen BC, Dziunycz P, Ristorcelli E, Ryan RJ, Ozuysal OY, et al. IRF6 is a mediator of Notch pro-differentiation and tumour suppressive function in keratinocytes. EMBO J. 2011;30(22):4571-85. doi: 10.1038/emboj.2011.325. PubMed PMID: 21909072; PubMed Central PMCID: PMCPMC3243593.
16. Slattery ML, Lundgreen A, Bondurant KL, Wolff RK. Interferon-signaling pathway: associations with colon and rectal cancer risk and subsequent survival. Carcinogenesis. 2011;32(11):1660-7. doi: 10.1093/carcin/bgr189. PubMed PMID: 21859832; PubMed Central PMCID: PMCPMC3204348.
17. Zengin T, Ekinci B, Kucukkose C, Yalcin-Ozuysal O. IRF6 Is Involved in the Regulation of Cell Proliferation and Transformation in MCF10A Cells Downstream of Notch Signaling. PLoS One. 2015;10(7):e0132757. doi: 10.1371/journal.pone.0132757. PubMed PMID: 26161746; PubMed Central PMCID: PMCPMC4498616.
18. de Freitas EM, Machado RA, de Moura Santos E, de Matos FR, Galvao HC, Miranda Soares PB, et al. Polymorphisms associated with oral clefts as potential susceptibility markers for oral and breast cancer. Arch Oral Biol. 2019;99:9-14. doi: 10.1016/j.archoralbio.2018.12.004. PubMed PMID: 30579133.
19. Botti E, Spallone G, Moretti F, Marinari B, Pinetti V, Galanti S, et al. Developmental factor IRF6 exhibits tumor suppressor activity in squamous cell carcinomas. Proc Natl Acad Sci U S A. 2011;108(33):13710-5. doi: 10.1073/pnas.1110931108. PubMed PMID: 21807998; PubMed Central PMCID: PMCPMC3158164.
20. Saito K, Ohta S, Kawakami Y, Yoshida K, Toda M. Functional analysis of KIF20A, a potential immunotherapeutic target for glioma. J Neurooncol. 2017;132(1):63-74. doi: 10.1007/s11060-016-2360-1. PubMed PMID: 28070829.
21. Rath O, Kozielski F. Kinesins and cancer. Nat Rev Cancer. 2012;12(8):527-39. doi: 10.1038/nrc3310. PubMed PMID: 22825217.

Figures

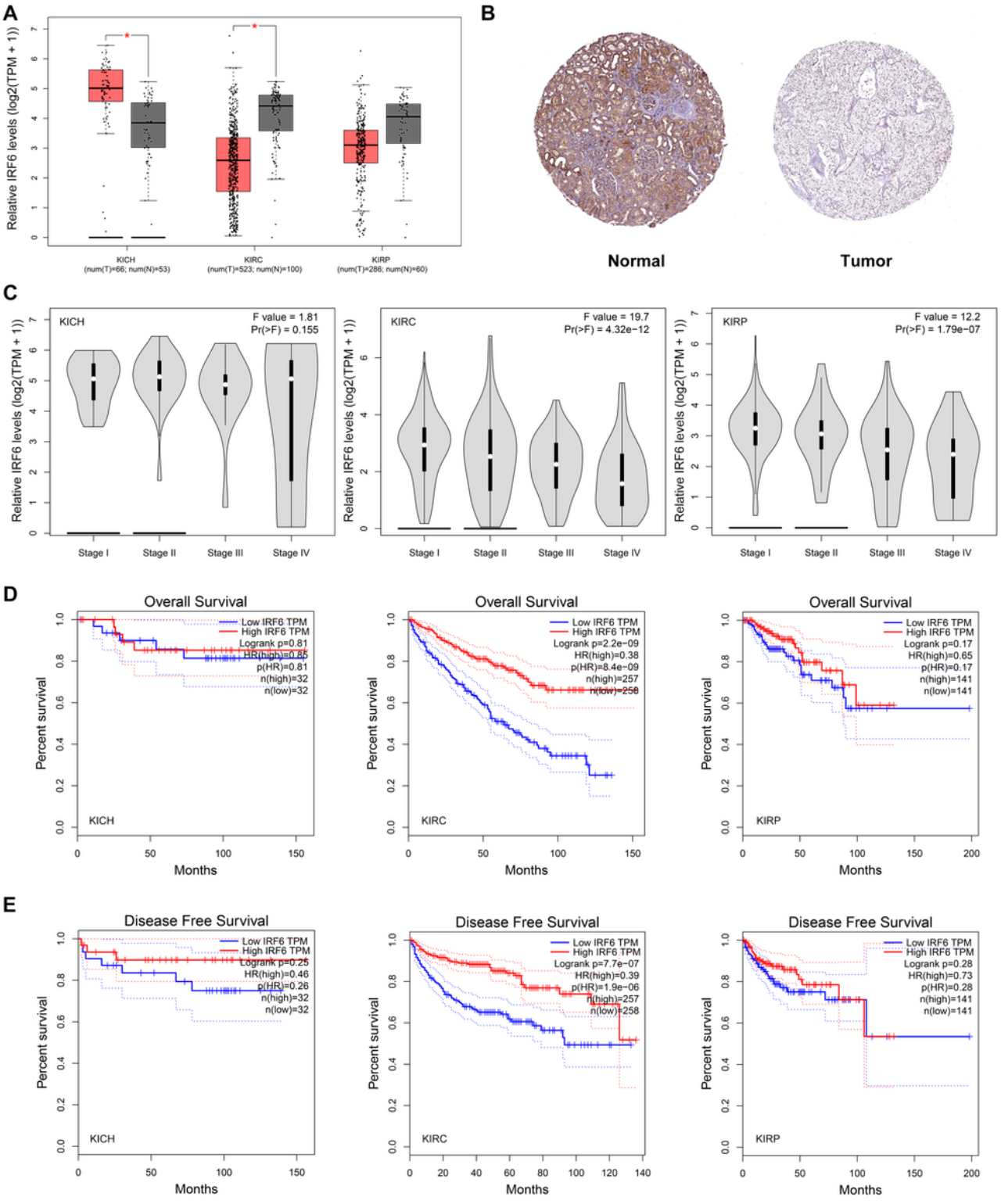

Figure 1

Expression of IRF6 in renal carcinoma tissues and its relationship with prognosis. A Validation of the gene expression levels of IRF6 between normal kidney and ccRCC samples based on TCGA data in GEPIA. . C. Validation of the correlation between the expression levels of IRF6 and the pathologic stage of ccRCC. D. Overall survival analysis of IRF6 in ccRCC (based on TCGA data in GEPIA). E. Disease free

survival analysis of IRF6 in ccRCC (based on TCGA data in GEPIA). Red line represented the samples with gene highly expressed and blue line was for the samples with gene lowly expressed. HR: hazard ratio.

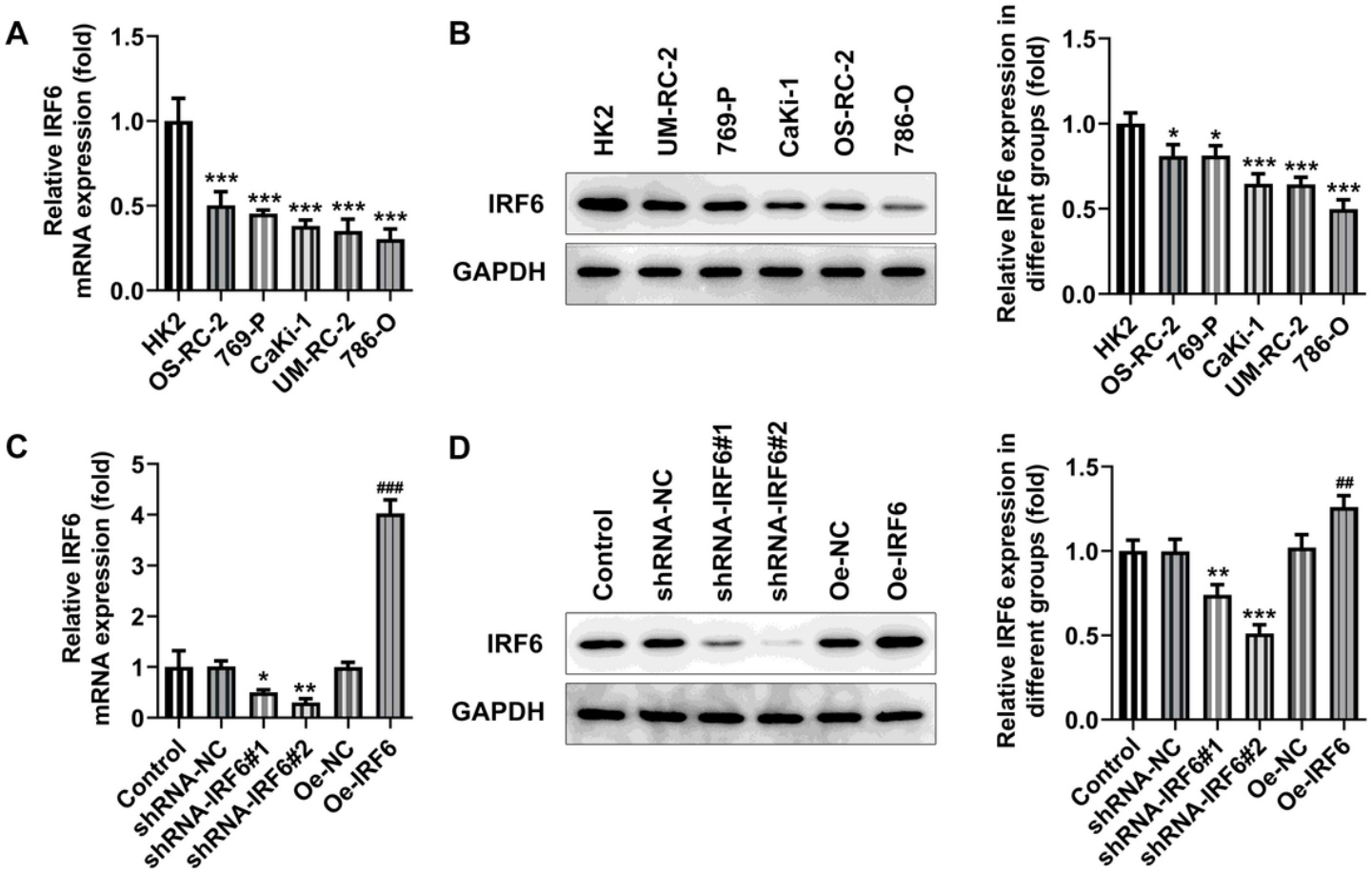

Figure 2

Expression of IRF6 in lung cancer cell lines. A. RT-qPCR detected the expression of IRF6 in different lung cancer cell lines. B. Western blot detected the expression of IRF6 in different lung cancer cell lines. *P<0.05, ***P<0.001 vs HK2. C. The expression of IRF6 in cells was detected by RT-qPCR after cell transfection. D. The expression of IRF6 in cells was detected by western blot after cell transfection. *P<0.05, **P<0.01, ***P<0.001 vs shRNA-NC. ## P<0.01, ### P<0.001 vs Oe-NC.

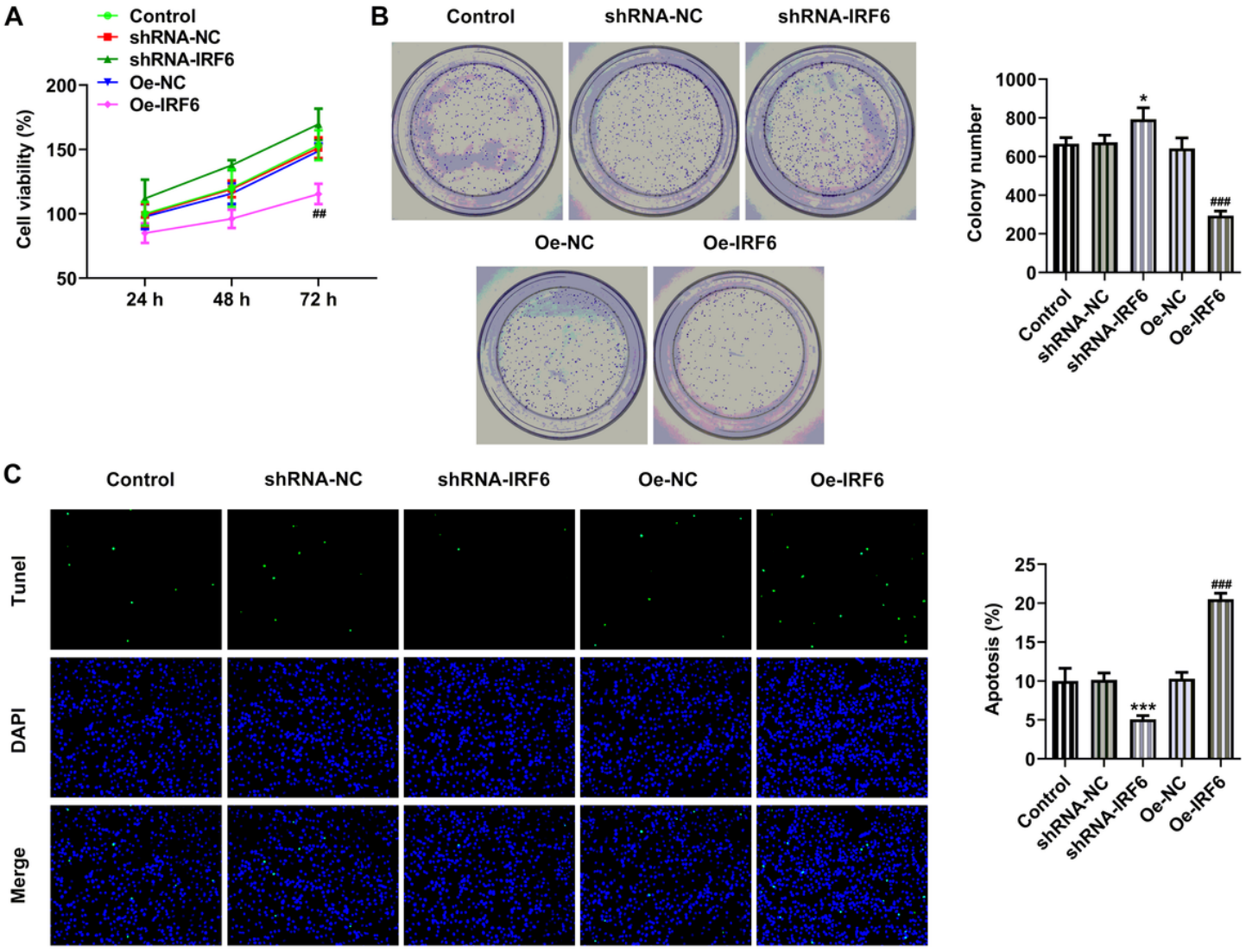

Figure 3

Overexpression of IRF6 inhibits proliferation of ccRCC cells. A. CCK-8 detected the cell viability. B. Clone formation assay detected the cell reproductive capacity. C. TUNEL assay detected the apoptosis of cells. *P<0.05, ***P<0.001 vs shRNA-NC. ### P<0.001 vs Oe-NC.

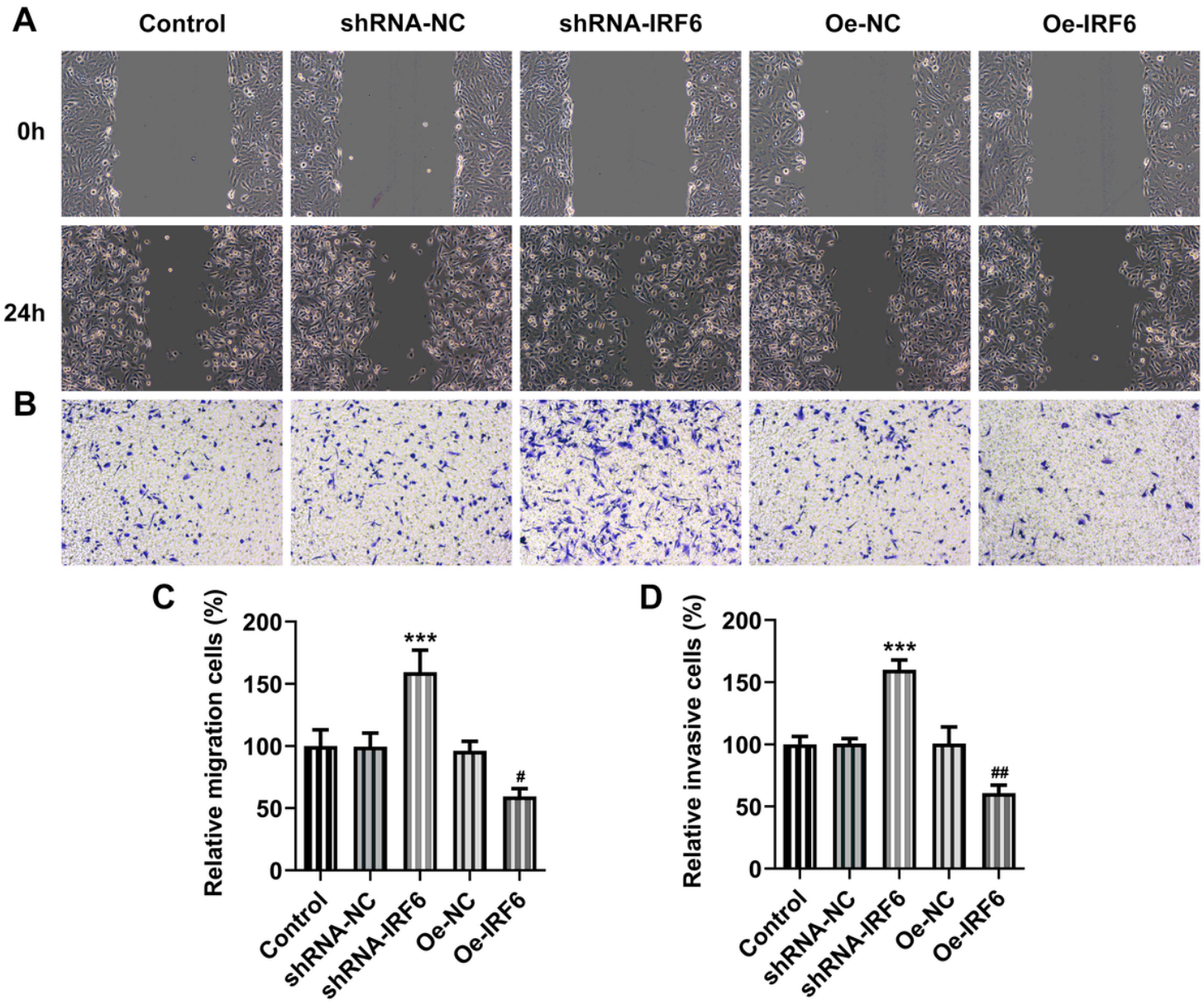

Figure 4

Overexpression of IRF6 inhibits invasion and migration of ccRCC cells. A. Wound healing detected the cell migration ability. B. Transwell detected the cell invasion ability. C. Statistical chart of cell mobility. D. Statistical chart of cell invasion. ***P<0.001 vs shRNA-NC. # P<0.05, ## P<0.01 vs Oe-NC.

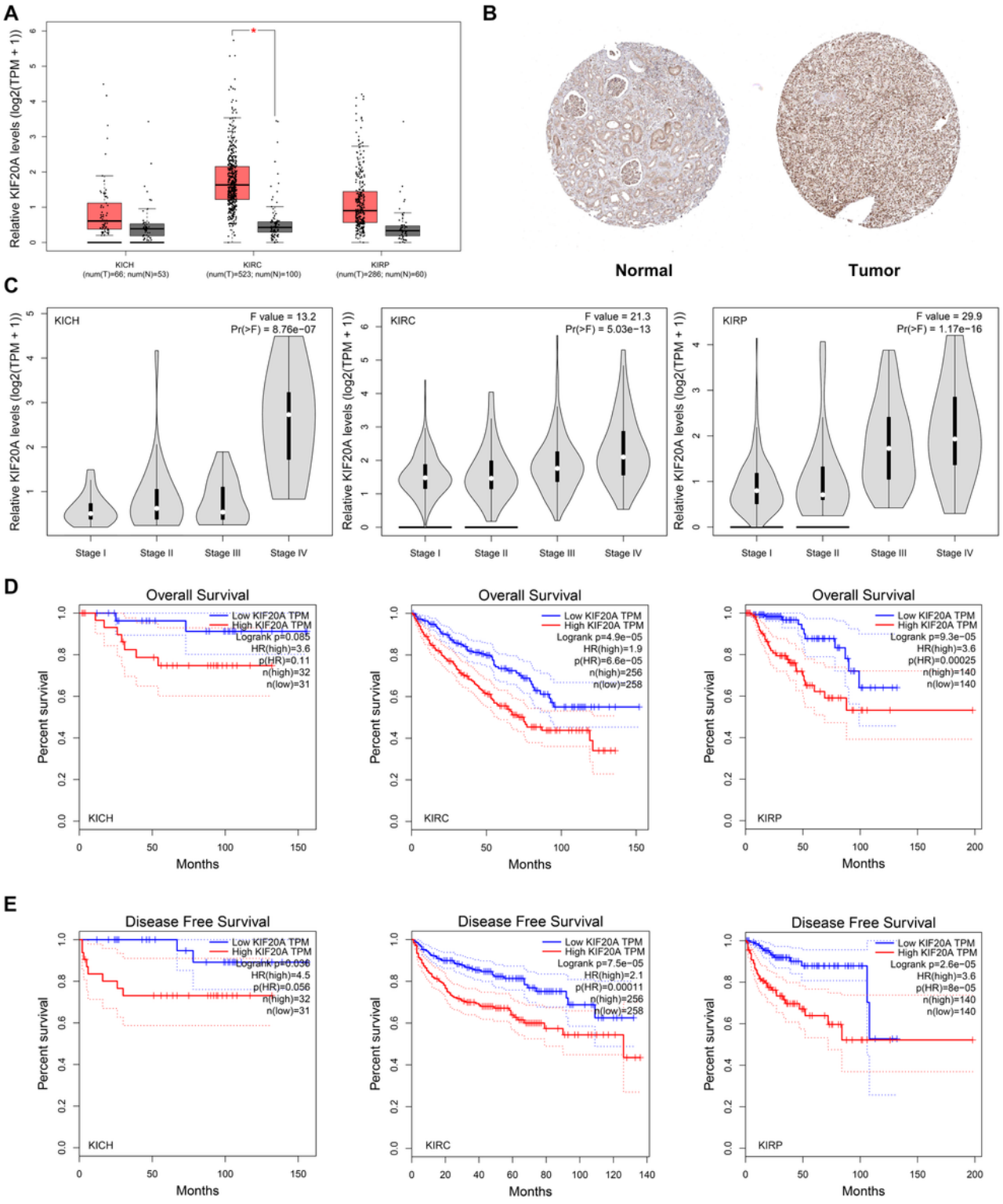

Figure 5

Expression of KIF20A in renal carcinoma tissues and its relationship with prognosis. A. Validation of the gene expression levels of KIF20A between normal kidney and ccRCC samples based on TCGA data in GEPIA. B. IHC staining of KIF20A expression in lung cancer tissues and in normal lung tissue. C. Validation of the correlation between the expression levels of KIF20A and the pathologic stage of ccRCC. D. Overall survival analysis of KIF20A in ccRCC (based on TCGA data in GEPIA). E. Disease free survival

analysis of KIF20A in ccRCC (based on TCGA data in GEPIA). Red line represented the samples with gene highly expressed and blue line was for the samples with gene lowly expressed. HR: hazard ratio.

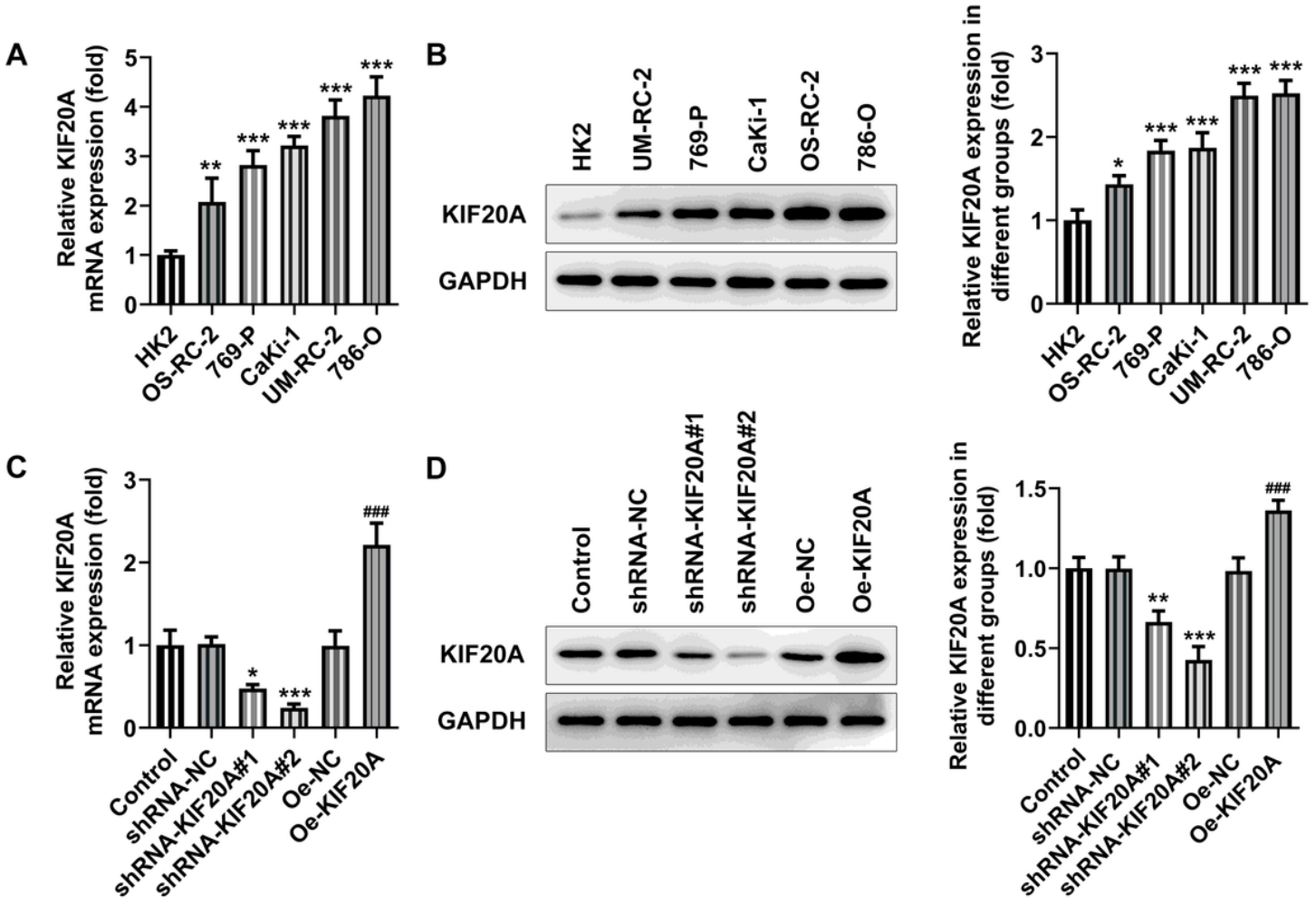

Figure 6

Expression of KIF20A in lung cancer cell lines. A. RT-qPCR detected the expression of KIF20A in different lung cancer cell lines. B. Western blot detected the expression of KIF20A in different lung cancer cell lines. *P<0.05, ***P<0.001 vs HK2. C. The expression of IRF6 in cells was detected by RT-qPCR after cell transfection. D. The expression of KIF20A in cells was detected by western blot after cell transfection. *P<0.05, **P<0.01, ***P<0.001 vs shRNA-NC. ## P<0.01, ### P<0.001 vs Oe-NC.

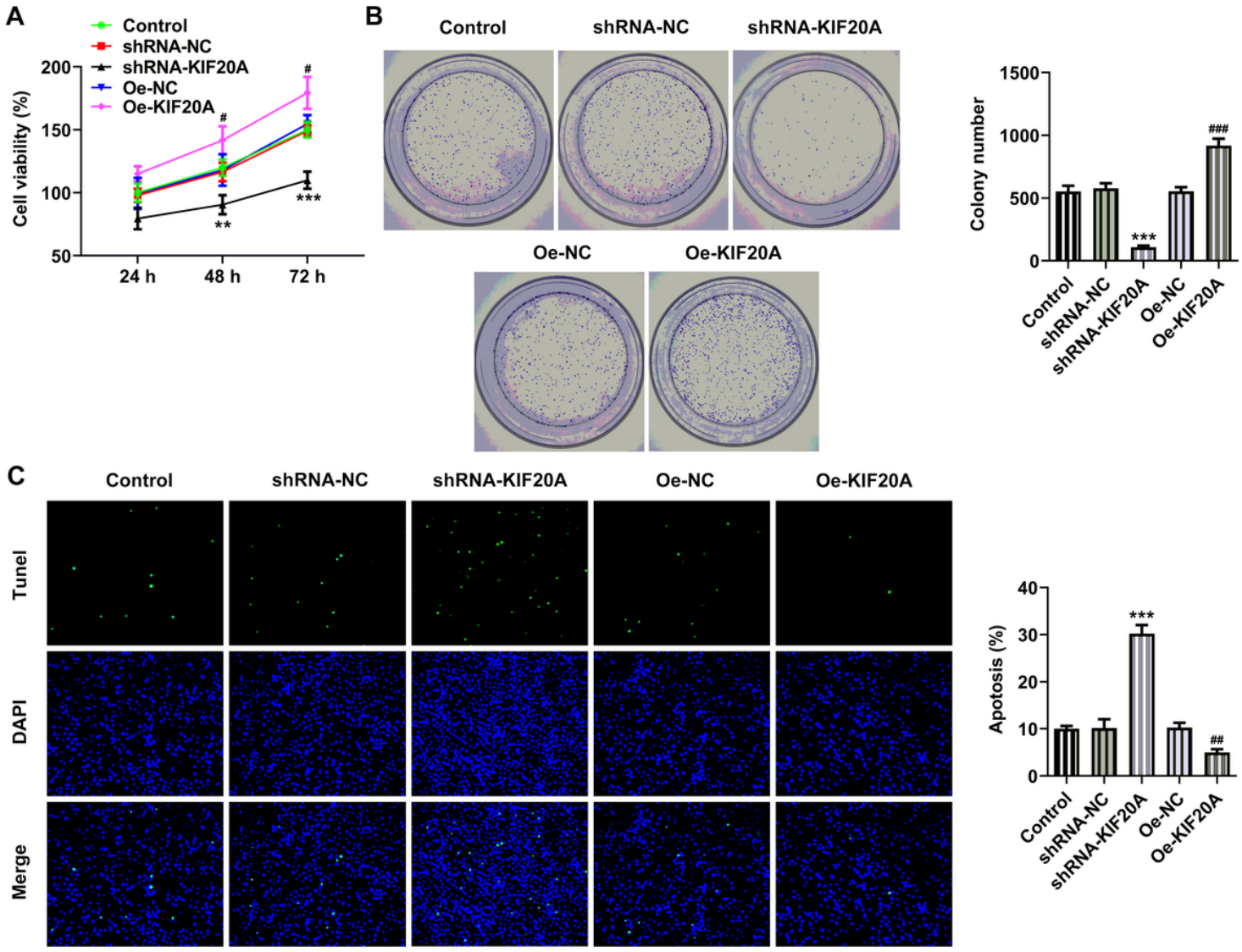

Figure 7

Interference with KIF20A inhibits proliferation of ccRCC cells. A. CCK-8 detected the cell viability. B. Clone formation assay detected the cell reproductive capacity. C. TUNEL assay detected the apoptosis of cells. *P<0.05, ***P<0.001 vs shRNA-NC. # P<0.05, ## P<0.01, ### P<0.001 vs Oe-NC.

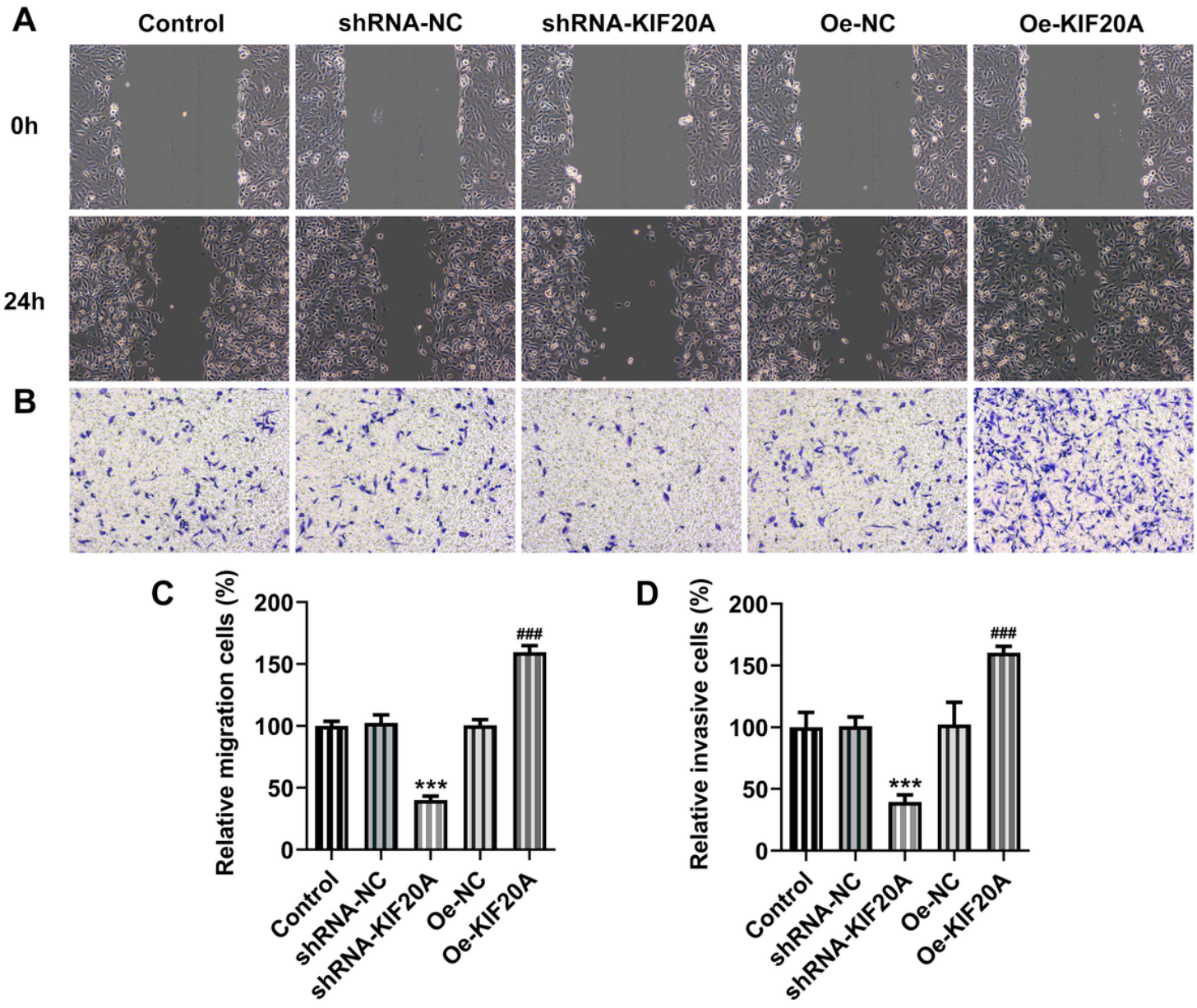

Figure 8

Overexpression of KIF20A inhibits invasion and migration of ccRCC cells. A. Wound healing detected the cell migration ability. B. Transwell detected the cell invasion ability. C. Statistical chart of cell mobility. D. Statistical chart of cell invasion. ***P<0.001 vs shRNA-NC. ### P<0.001 vs Oe-NC.

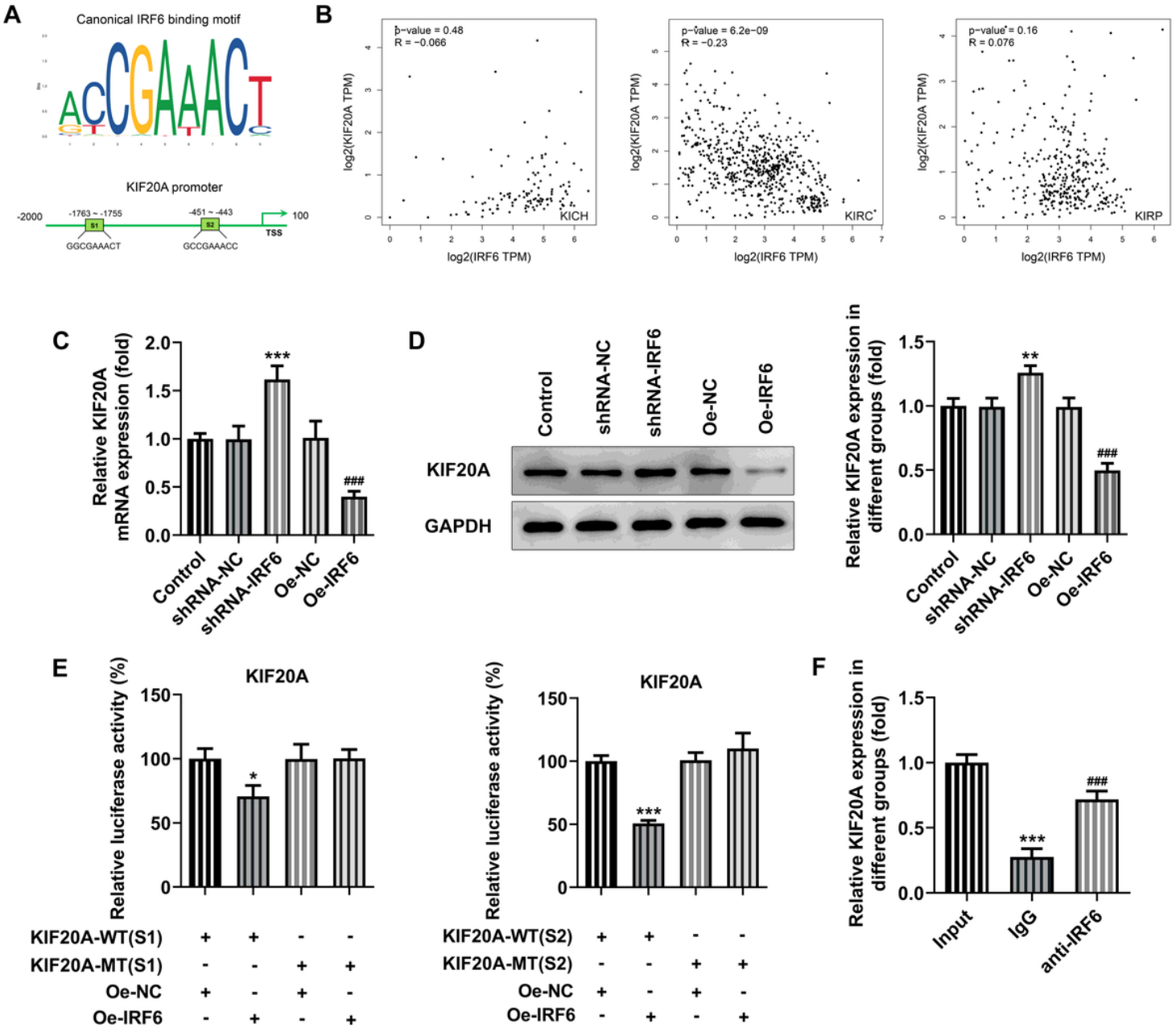

Figure 9

IRF6 directly binds to the KIF20A promoter to regulate KIF20A expression. A. JASPAR database predicts binding sites between IRF6 and KIF20A. B. Correlation between IRF6 and KIF20A expression in ccRCC. C. RT-qPCR detected the expression of KIF20A. D. Western blot detected the expression of KIF20A. **P<0.01, ***P<0.001 vs shRNA-NC. ### P<0.001 vs Oe-NC. E. Luciferase was used to detect the transcriptional activity of KIF20A promoter mutant in ccRCC cells. *P<0.05 vs KIF20A-WT+Oe-IRF6. F. ChIP verified that IRF6 binds to the KIF20A promoter. ***P<0.001 vs Input. ### P<0.001 vs IgG.

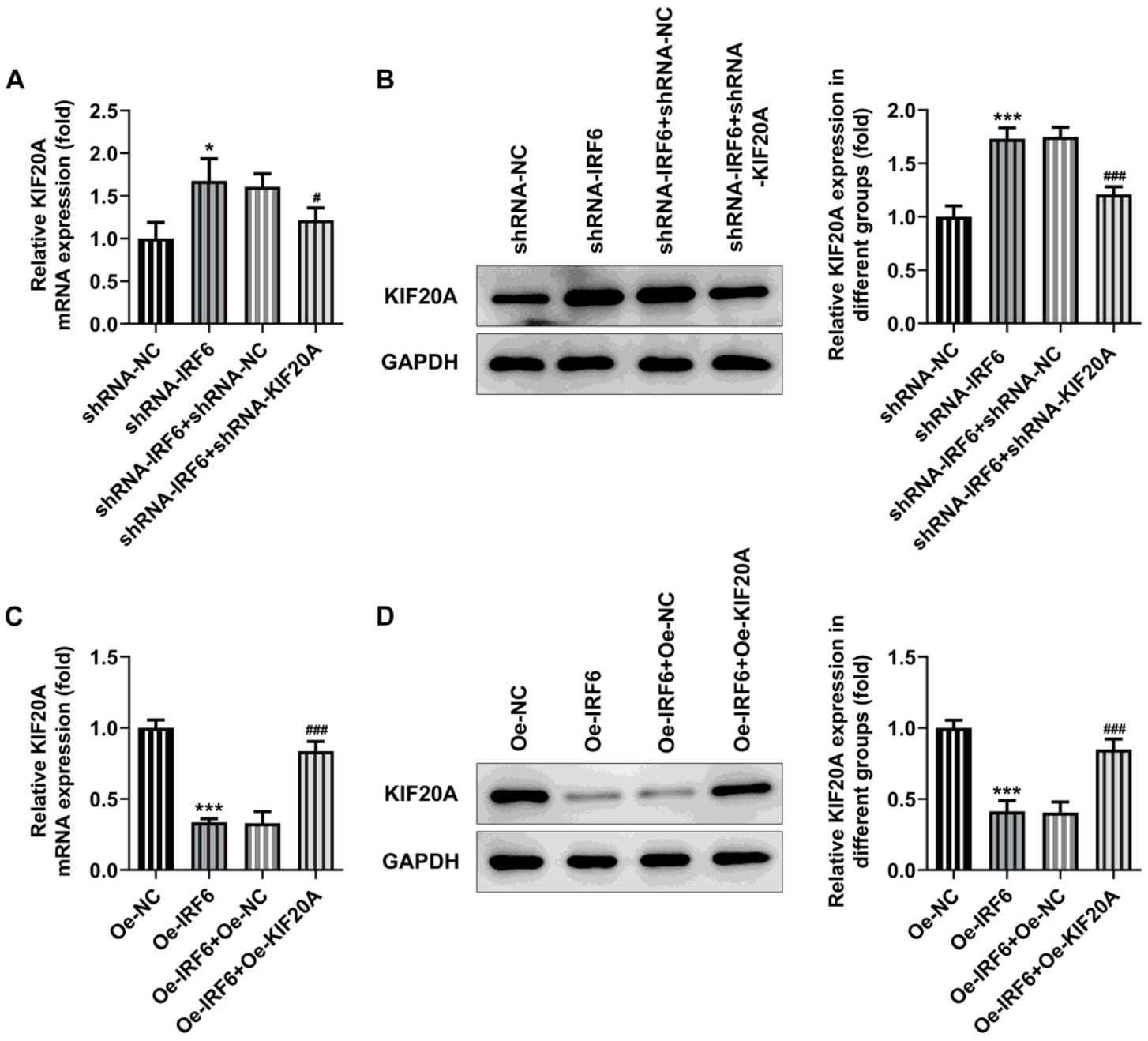

Figure 10

Expression of KIF20A after cell transfection. A. RT-qPCR detected the expression of KIF20A after inhibition of IRF6 and KIF20A expression. B. Western blot detected the expression of KIF20A after inhibition of IRF6 and KIF20A expression. *P<0.05, ***P<0.001 vs shRNA-NC. #P<0.05, ###P<0.001 vs shRNA-IRF6 + shRNA-NC. C. RT-qPCR detected the expression of KIF20A after overexpression of IRF6 and KIF20A. D. Western blot detected the expression of KIF20A after overexpression of IRF6 and KIF20A. ***P<0.001 vs Oe-NC. ### P<0.001 vs Oe-IRF6 + Oe-NC.

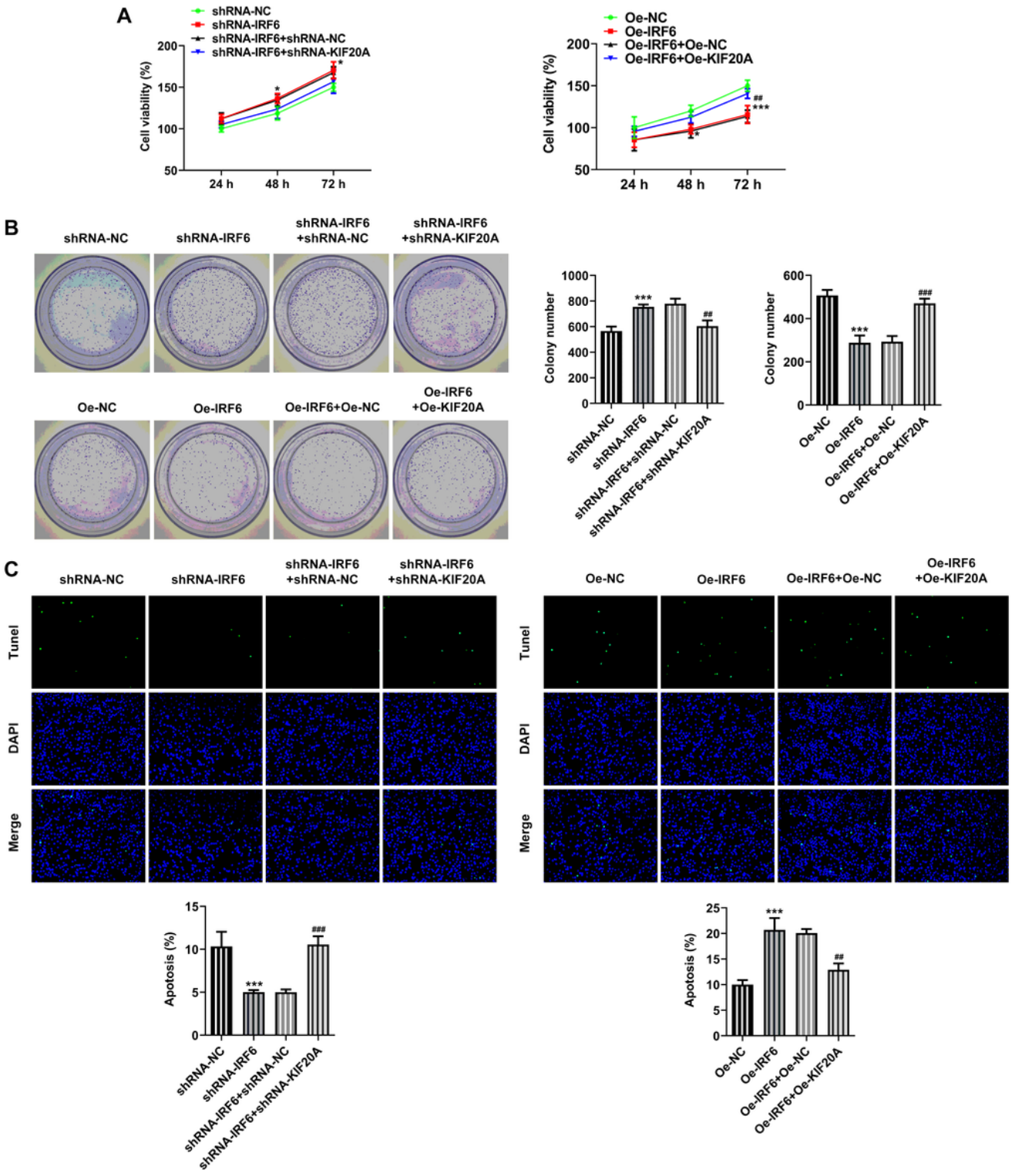

Figure 11

KIF20A partially reverses the effects of IRF6 on the proliferation of ccRCC cells. A. CCK-8 detected the cell viability. B. Clone formation assay detected the cell reproductive capacity. C. TUNEL assay detected the apoptosis of cells. *P<0.05, ***P<0.001 vs Oe-NC. ##P<0.01, ### P<0.001 vs Oe-IRF6 + Oe-NC.

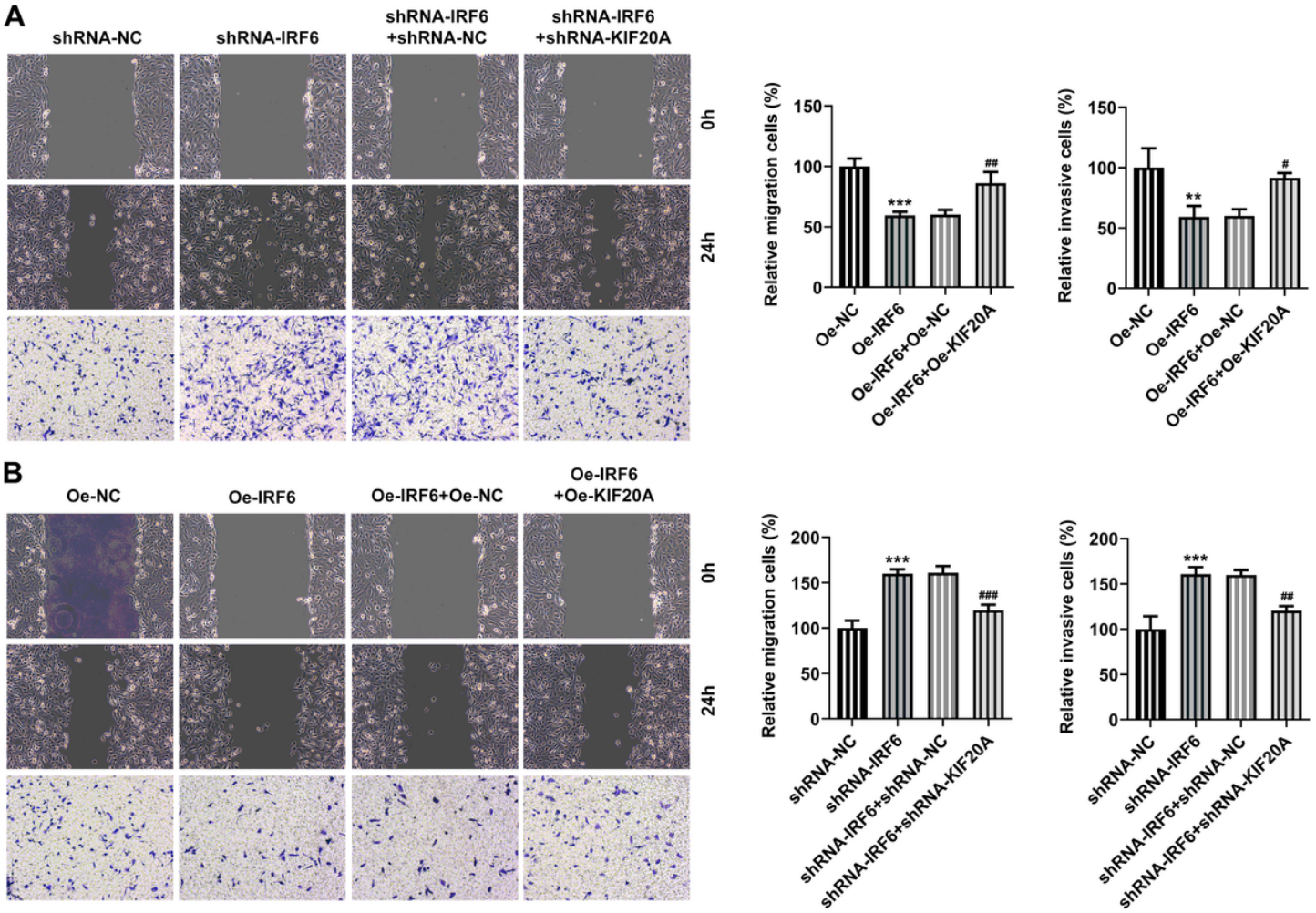

Figure 12

KIF20A partially reverses the effects of IRF6 on the invasion and migration of ccRCC cells. A. Wound healing detected the cell migration ability. B. Transwell detected the cell invasion ability. **P<0.01, ***P<0.001 vs Oe-NC. #P<0.05, ##P<0.01, ### P<0.001 vs Oe-IRF6 + Oe-NC.

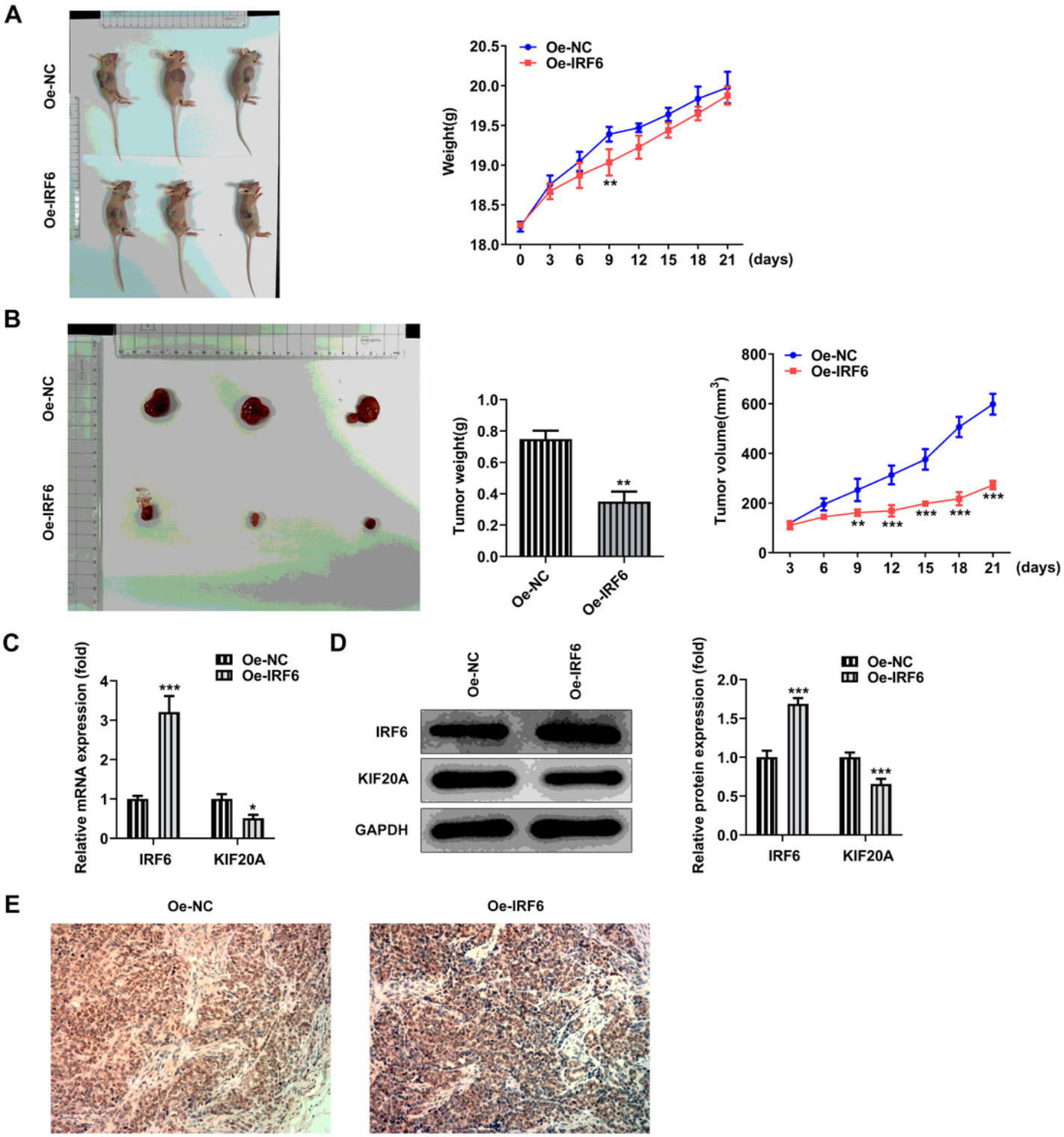

Figure 13

Overexpression of IRF6 inhibits the growth and metastasis of ccRCC in vivo. A. Mice were weighed and photographed before treatment. B. The weight and volume of tumor tissue. C. RT-qPCR detected the expression of IRF6. D. Western blot detected the expression of IRF6. E. The expression of ki-67 in tumor tissues was detected by IHC.